



Detection of Building Boundaries in Mine Fields using Wavelet Method

Ali Muhittin ALBORA

Istanbul University, Engineering Faculty, Geophysical Department, 34320, Avcilar, Istanbul, Turkey

Abstract In geophysical engineering analysis of the data measured in the field is very important. In the case of potential sources, the wavelet method distinguishes particularly between regional (effects of deeper masses) and residual (effects of near-surface masses). We can think of this as noise analysis. The consequences of undesirable effects on geophysical data are loud for us. If the residual area is required according to the working area, the regional effect on the map obtained here is a disturbing effect for us. This effect must be discarded and the wavelet method is well suited for this task. In this study, synthetic data were distinguished and applied on mine fields as a field study. An important feature of geophysical data is the detection of the boundaries of the underground structure that creates anomalies. For this purpose, the wavelet method can be applied to potential source areas to determine the structure boundaries. In particular, the boundaries of the structure can be determined using the wavelet method's detail coefficients. In boundary detection, we can determine the vertical bounds of the vertical component construction, the horizontal boundary of the horizontal component construction and the corners of the cross-component construction. In this study, the success of the wavelet method is tested on the synthetic samples and then the map of the chromite anomaly map is interpreted as the land data.

Keywords Turkey-Elazığ-Gölalan region, Wavelet Transform, Chrome mine, Gravity anomaly

Introduction

First, in 1909, wavelet method was used in Haar's thesis. The most important feature of the Haar wavelet function is its tight support. On the other hand, the Haar wavelet function does not always have a derivative. After the 1930's, the wavelet method has been developed by many scientists and has been widely used. In recent years, the wavelet method, which takes the place of the Fourier spectrum in geophysical engineering, has many applications. As is known, two and three dimensional filter studies can be performed using the wavelet method [1-10]. In this method, we can use various coefficients and the residual structure can be found as much as the desired number of repetitions. Another important feature of the wavelet method is that the horizontal, vertical and diagonal outputs of the residual anomaly map that we want to obtain can be found. Some authors have also noticed the success of the Wavelet method in terms of boundary detection and the performance of the Cellular Neural Network method in terms of boundary detection. A new method called Wave-CNN has been introduced [11], [12] and [13]. The boundaries of the chrome ore were tried to be determined by using the gravite method in Elazığ-Gölalan region, which was chosen as the study site.

Materials and Methods: Wavelet Transforms

The classes of functions that present the wavelet transform are those that are square integrable on the real line. This class is denoted as $L^2(R)$,



$$f(x) \in L^2(R) \Rightarrow \int_{-\infty}^{+\infty} |f(x)|^2 dx < \infty. \quad (1)$$

The set of functions that are generated in the wavelet analysis are obtained by dilating (scaling) and translating (time shifting) a single prototype function, which is called the mother wavelet. The wavelet function $\psi(x) \in L^2(R)$ has two characteristic parameters, called dilation a and translation b , which vary continuously.

A set of wavelet basis function $\psi_{a,b}(x)$ may be given as

$$\psi_{a,b}(x) = \frac{1}{\sqrt{|a|}} \psi\left(\frac{x-b}{a}\right) \quad a, b \in R; a \neq 0. \quad (2)$$

Here, the translation parameter, b , controls the position of the wavelet in time. The “narrow” wavelet can access high frequency information, while the more dilated wavelet can access low frequency information. This means that the parameter a , varies for different frequencies. The continuous wavelet transform is defined by

$$W_{a,b}(f) = \langle f, \psi_{a,b} \rangle = \int_{-\infty}^{+\infty} f(x) \psi_{a,b}(x) dx. \quad (3)$$

The wavelet coefficients are given as the inner product of the function being transformed with each basis function.

[4] invented one of the most elegant families of wavelets. They are called compactly supported orthonormal wavelets, which are used in discrete wavelet transform (DWT). In this approach, the scaling function is used to compute the ψ . The scaling function $\phi(x)$ and the corresponding wavelet $\psi(x)$ are defined by

$$\phi(x) = \sum_{k=0}^{N-1} c_k \phi(2x - k), \quad (4)$$

$$\psi(x) = \sum_{k=0}^{N-1} (-1)^k c_k \phi(2x + k - N + 1), \quad (5)$$

where N is an even number of wavelet coefficients c_k , $k=0$ to $N-1$. The discrete presentation of an orthonormal compactly supported wavelet basis of $L^2(R)$ is formed by dilation and translation of signal function $\psi(x)$, called the wavelet function. Assuming that the dilation parameters a and b take only discrete values. $a = a_0^j$, $b = kb_0 a_0^j$. Where $k, j \in Z$, $a_0 > 1$, and $b_0 > 0$ [4]. The wavelet function may be rewritten as

$$\psi_{j,k}(x) = a_0^{-j/2} \psi(a_0^{-j} x - kb_0), \quad (6)$$

and, the discrete-parameter wavelet transform (DPWT) is defined as

$$DPWT(f) = \langle f, \psi_{j,k} \rangle = \int_{-\infty}^{+\infty} f(x) a_0^{-j/2} \psi(a_0^{-j} x - kb_0) dx, \quad (7)$$

The dilations and translations are chosen based on power of two, so called dyadic scales and positions, which make the analysis efficient and accurate. In this case, the frequency axis is partitioned into bands by using the power of two for the scale parameter a . Considering samples at the dyadic values, one may get $b_0 = 1$ and $a_0 = 2$, and then the discrete wavelet transform becomes,

$$DPWT(f) = \langle f, \psi_{j,k} \rangle = \int_{-\infty}^{+\infty} f(x) \{2^{-j/2} \psi(2^{-j} x - k)\} dx. \quad (8)$$

Here, $\psi_{j,k}(x)$ is defined as,

$$\psi_{j,k}(x) = 2^{-j/2} \psi(2^{-j} x - k), \quad j, k \in Z. \quad (9)$$



Multi-resolution Analysis (MRA)

[14] introduced an efficient algorithm to perform the DPWT known as the Multi-resolution Analysis (MRA). It is well known in the signal processing area as the two-channel sub-band coder. The MRA of $L^2(R)$ consists of successive approximations of the space V_j of $L^2(R)$. There exist a scaling function $\phi(x) \in V_0$ such that,

$$\phi_{j,k}(x) = 2^{-j/2} \phi(2^{-j}x - k); \quad j, k \in \mathbb{Z}. \quad (10)$$

For the scaling function $\phi(x) \in V_0 \subset V_1$, there is a sequence $\{h_k\}$,

$$\phi(x) = 2 \sum_k h_k \phi(2x - k). \quad (11)$$

This equation is known as two-scale difference equation. Furthermore, let us define W_j as a complementary space of V_j in V_{j+1} , such that $V_{j+1} = V_j \oplus W_j$ and $\bigoplus_{j=-\infty}^{+\infty} W_j = L^2(R)$. Since the $\psi(x)$ is a wavelet and it is also an element of V_0 , a sequence $\{g_k\}$ exists such that,

$$\psi(x) = 2 \sum_k g_k \phi(2x - k). \quad (12)$$

It is concluded that the multi-scale representation of a signal $f(x)$ may be achieved in different scales of the frequency domain by means of an orthogonal family of functions $\phi(x)$. Now, let us show how to compute the function in V_j [14]. The projection of the signal $f(x) \in V_0$ on V_j defined by $P_v f^i(x)$ is given by,

$$P_v f^i(x) = \sum_k c_{j,k} \phi_{j,k}(x). \quad (13)$$

Here, $c_{j,k} = \langle f, \phi_{j,k}(x) \rangle$. Similarly, the projection of the function $f(x)$ on the subspace W_j is also defined by,

$$P_w f^j(x) = \sum_k d_{j,k} \psi_{j,k}(x), \quad (14)$$

where $d_{j,k} = \langle f, \psi_{j,k}(x) \rangle$. Because of $V_j = V_{j-1} \oplus W_{j-1}$, the original function $f(x) \in V_0$ can be rewritten as,

$$f(x) = \sum_k c_{j,k} \phi_{j,k}(x) + \sum_j \sum_k d_{j,k} \psi_{j,k}(x) \quad J > j_0. \quad (15)$$

The coefficients $c_{j,k}$ and $d_{j,k}$ are given by,

$$c_{j-1,k} = \sqrt{2} \sum_i h_{i-2k} c_{j,k}, \quad (16)$$

and

$$d_{j,k} = \sqrt{2} \sum_j g_{j-2k} c_{j,k}. \quad (17)$$

The multi-resolution representation is linked to Finite Impulse Response (FIR) filters. The scaling function ϕ and the wavelet ψ are obtained using the filter theory and consequently also the coefficients are defined by these last two equations. If at $x=t/2$, $F\{\phi(x)\}$ is considered and

$$\Phi(\omega) = H\left(\frac{\omega}{2}\right) \Phi\left(\frac{\omega}{2}\right), \quad (18)$$

As $\phi(0) \neq 0$, $H(0)=1$, this means that $H(\omega)$ is a low-pass filter. According to this result $\phi(t)$ is computed by the low-pass filter $H(\omega)$. The mother wavelet $\psi(t)$ is computed by defining the function $G(\omega)$ so that



$H(\omega)G^*(\omega) + H(\omega + \pi)G^*(\omega + \pi) = 0$. Here, $H(\omega)$ and $G(\omega)$ are quadrature mirror filters for MRA solution,

$$G(\omega) = -\exp(-j\omega)H^*(\omega + \pi). \tag{19}$$

Substituting $H(0)=1$ and $H(\pi)=0$, it yields $G(0)=0$ and $G(\pi)=1$, respectively. This means that $G(\omega)$ is a high pass filter. As a result, the MRA is a kind of two-channel sub-band coder used in the high-pass and low-pass filters, from which the original signal can be reconstructed.

Since a major potential application of wavelets is in image processing, 2-D wavelet transform is a necessity. The subject, however, is still in an evolving stage and this section will discuss only the extension of 1-D wavelets to the 2-D case. The idea is to first form a 1-D sequence from the 2-D image row sequences, do a 1-D MRA, restore the MRA outputs to a 2-D format and repeat another MRA to the 1-D column sequences. The two steps of restoring to a 2-D sequence and forming a 1-D column sequence can be combined efficiently by appropriately selecting the proper points directly from the 1-D MRA outputs. As seen in Figure 1, after the 1-D row MRA, each low-pass and high-pass output goes through a 2-D restoration and 1-D column formation process and then move on to another MRA. Let t_1 and t_2 , be the 2-D co-ordinates and $L=$ low-pass, $H=$ high-pass. Then the 2-D separable scaling function is,

$$\phi^{(1)}(t_1, t_2) = \phi(t_1)\phi(t_2), \quad LL \tag{22}$$

original signal can be reconstructed. Then 2-D separable wavelets are,

$$\psi^{(2)}(t_1, t_2) = \phi(t_1)\psi(t_2), \quad LH \tag{21}$$

$$\psi^{(3)}(t_1, t_2) = \psi(t_1)\phi(t_2), \quad HL \tag{22}$$

$$\psi^{(4)}(t_1, t_2) = \psi(t_1)\psi(t_2), \quad HH \tag{23}$$

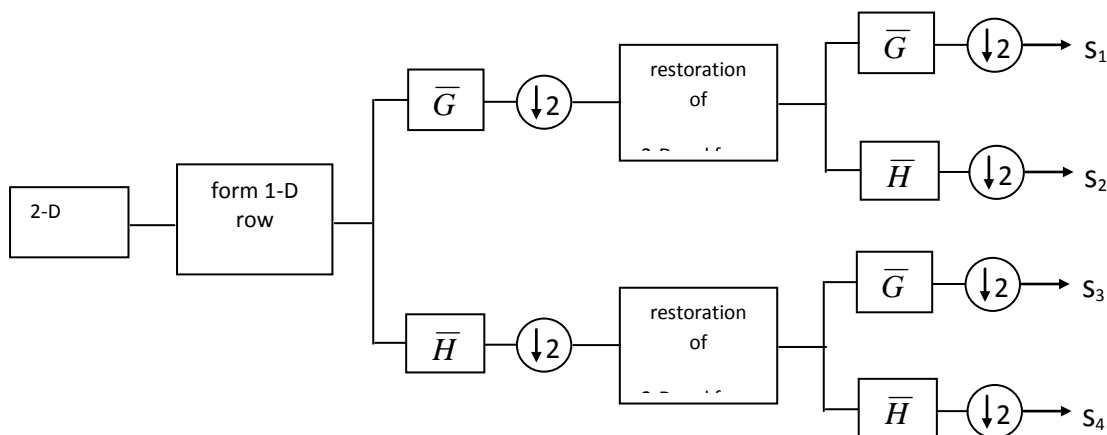


Figure 1: 2-D Multi-resolution Analysis (MRA) decomposition [8]

with the corresponding wavelet coefficients s_2 , s_3 and s_4 . It is easy to verify that the $\psi^{(i)}$ are orthonormal wavelets, i.e.,

$$\iint \psi^{(i)}(t_1, t_2) dt_1 dt_2 = 0, \tag{24}$$

$$\langle \psi_{mn}^{(i)}, \psi_{kl}^{(i)} \rangle = \delta_{m-k} \delta_{n-l}, \tag{25}$$

The scheme of separable 2-D processing, while simple and uses available 1-D filters, has disadvantages when compared to a genuine, 2-D MRA with non-separable filters. The latter possesses more freedom in design, can provide a better frequency and even linear phase response, and have non-rectangular sampling [8].

Synthetic Applications

Magnetic data observed in geophysical surveys are the sum of magnetic fields produced by all underground sources. In magnetic, this technique is better developed than in other methods because the theoretical analysis is straightforward. The targets for specific surveys are often small-scale structures buried at shallow depths, and these targets are embedded in a regional field that arises from residual sources that are usually larger or deeper than the targets or are located farther away. Correct estimation and removal of the regional field from initial field observations yields the residual field produced by the target sources.

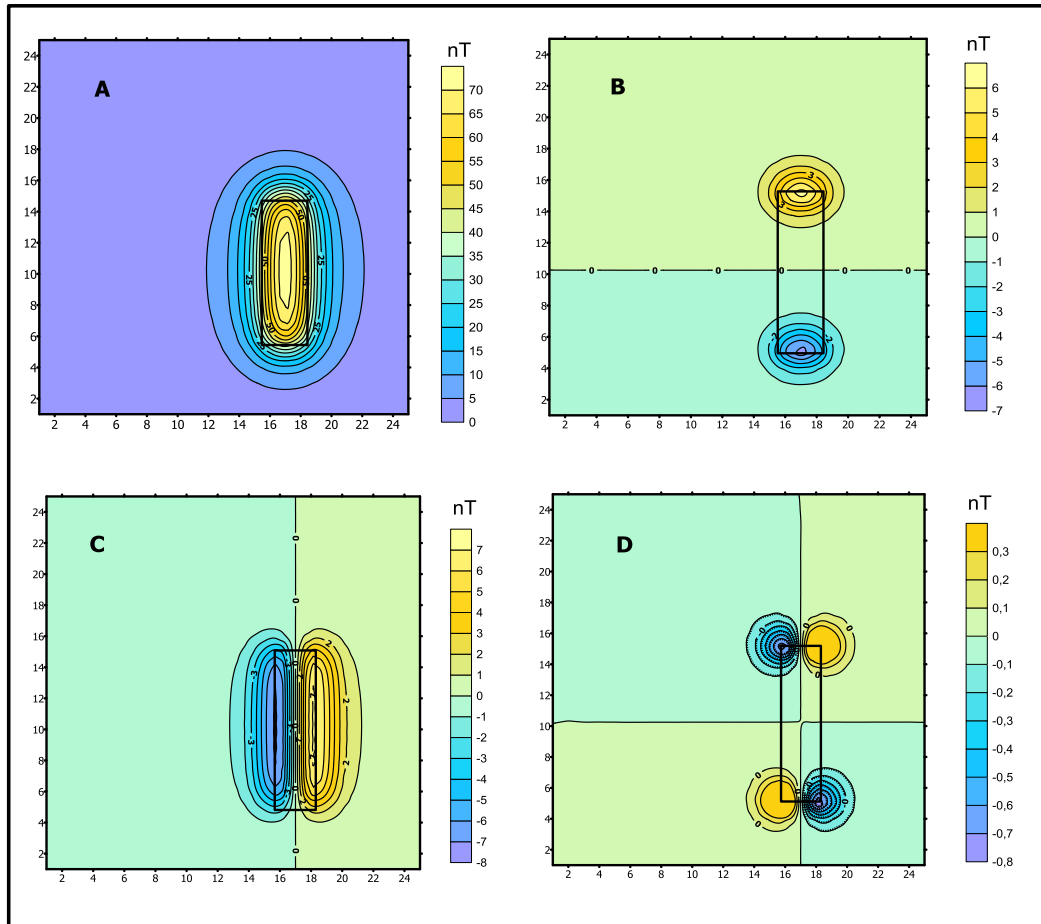


Figure 2: The horizontally placed prisms model (A) magnetic anomaly of the horizontally placed prisms model (B) horizontal component output. (C) vertical component output. (D) diagonal component output.

Interpretation and numerical modeling are carried out on the residual field data, and the reliability of the interpretation depends to a great extent upon the success of the regional-residual separation. A synthetic study as a solution of boundary detection problems is given in Figure 2a. Here a total magnetic anomaly of a two-dimensional prism is used. Rectangular prism selection is to reveal the ability of the intended wavelet algorithm to determine the boundary. In Fig. 2a, the detail coefficients of the wavelet method are applied to the synthetic prism model, and B, C, D, horizontal, diagonal and vertical wavelet components are obtained respectively. In Figure 2A, the prismatic structure is seen as a regional effect. Since there is no noise here, the input data and the output data are similar. At the output of the horizontal wavelet, there are negative and positive anomalies gathered at the horizontal boundaries (Figure 2b). The vertical output of the wavelength is given in Figure 2c. As in Figure 2b, negative and positive polarized anomalies are visible at the vertical borders. The centers of the Anomalies are precisely on the long edge prisms. In Figure 2d, similar polarized anomalies are seen at the corners and the anomalies are on the longer side of the central prism model.



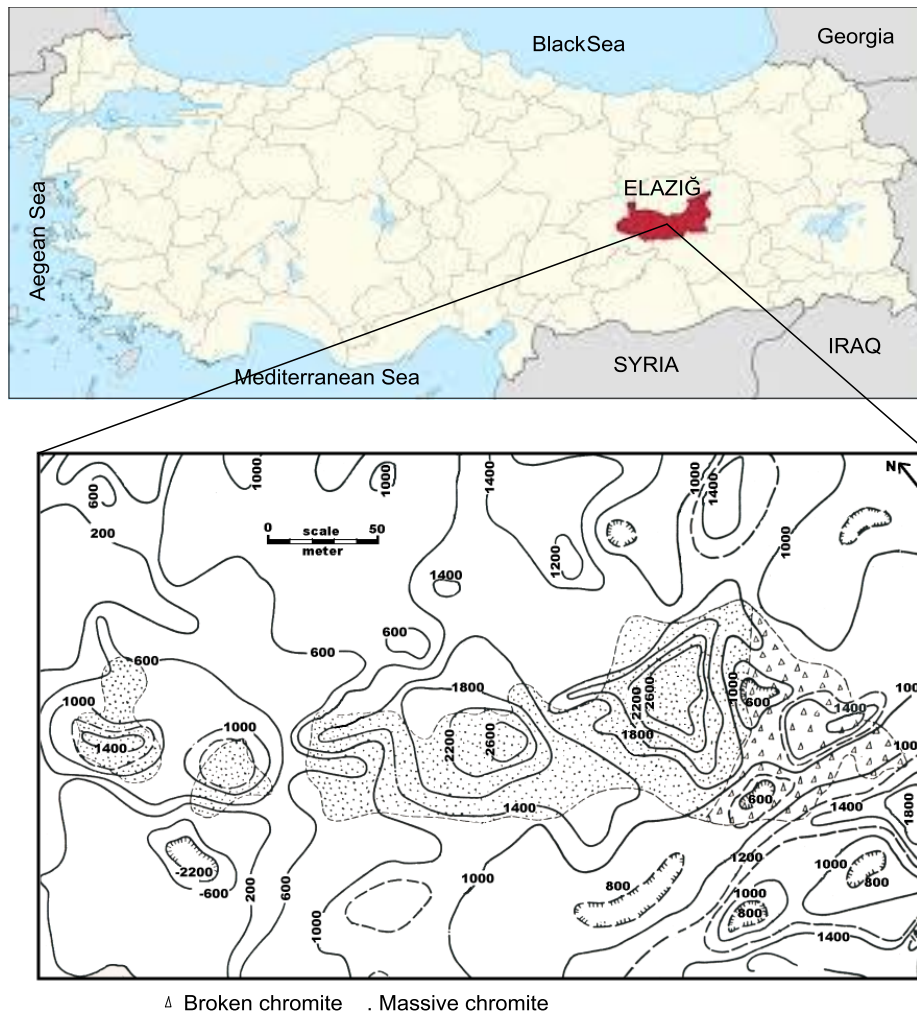


Figure 3: Turkey map a. the region of Elazığ shown in red b. Vertical magnetic anomaly map of chrome field in Golalan-Elazığ region [15].

Application of wavelet method to Elazığ-Gölalan chrome field

In the concessions of the Golalan chromate field works at the East of Turkey, chromate is found in the midst of a large region of igneous ultrabasic and basic rocks, usually in dunite serpentines, and sometimes in rhombic pyroxene serpentines of various degrees of alterations (Figure 3a). Extremely altered talc serpentine in the form of soft, gray, clay-like material, is found under some of these chromate masses, so that the chromate appears to be floating on this material. The known and exploited chromate deposits of this region are among the largest and richest chromate masses of the world. As a result of these surveys, chromate masses about 250.000 tons were found at the bottom of an open cut beneath a thin horizontal sheet of chromate. The considered mine city is at $39^{\circ} 28'$ East longitude and $38^{\circ} 28'$ North altitude and lies about 55 km East-Southeast of the city of Elazığ. Vertical magnetic anomaly map of Golalan chromate is given (Figure 3b). Positions of the chromate masses obtained by drilling data are shown in Figure 3b. Magnetic anomaly map is also located over Figure 3b. The three anomalies except the one on the right bottom in Figure 5, are all related with chromate masses [16]. The wavelet transform of the vertical magnetic anomaly map of the Gölalan-Elazığ region given in Figure 3b has been investigated. When looking at the wavelet transform, the residual anomaly map given in Figure 3a is obtained. There are more profound effects on the regional anomaly map. The wavelet components are shown in Figure 3b as horizontal component anomaly map, Figure 3c as vertical component map, and Figure 3d as cross component anomaly map. Horizontal discontinuities are observed in the wavelet horizontal component map. These discontinuities are marked by horizontal lines (3b). In the vertical component outputs, discontinuities in the vertical direction were

detected and plotted on the map (Figure 3c). At the cross-component outputs, corner points of the anomaly-forming structures are determined. These corners were combined to reveal building boundaries (figure 3d).

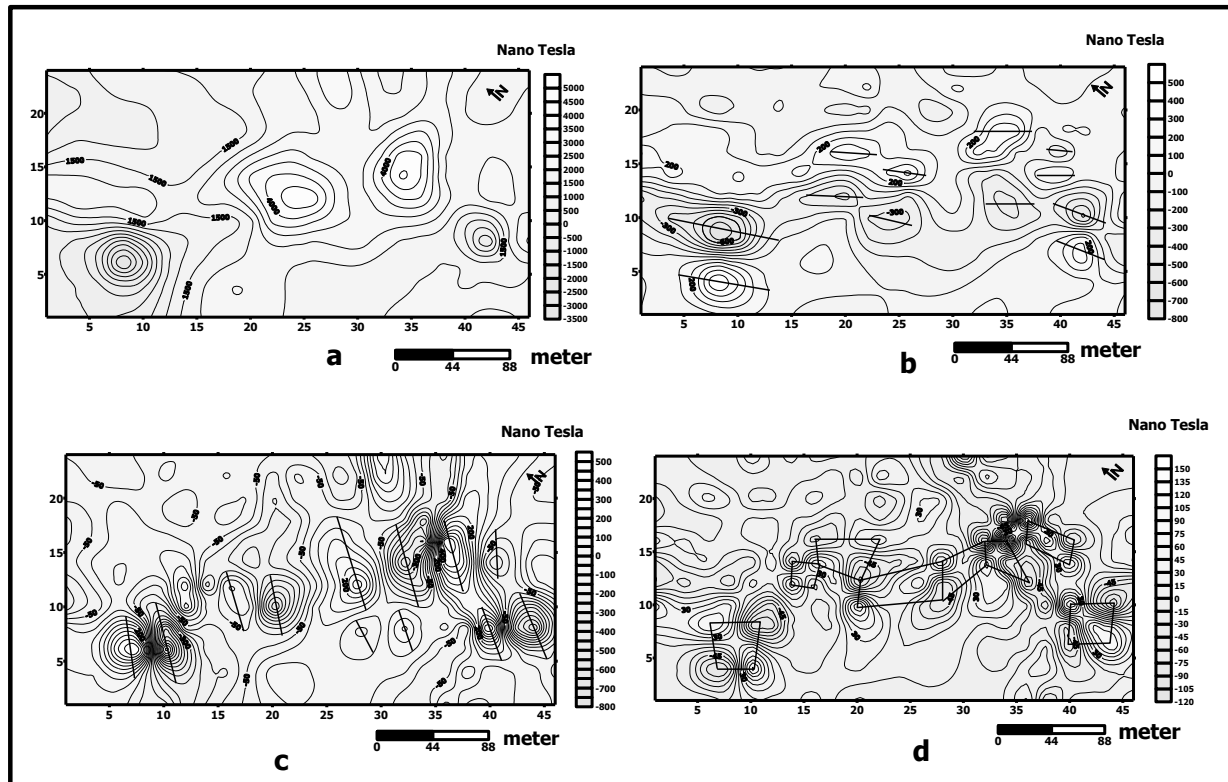


Figure 4: Golalan-Elazığ magnetic anomaly map a. Wavelet approach (Residual anomaly map, interval contour 250). b. horizontal component output of a (interval contour 100). c. vertical component output of a (interval contour 100). d. diagonal component output of a (interval contour 20).

Conclusion and Discussion

In this study, the success of the wavelet method in determining the boundaries of structure is investigated. The wavelet method was first tested on a magnetic anomaly map of a vertical prism. The aim here is to reveal the horizontal vertical and diagonal components of the prismatic structure (Figure 2). Then the map wavelets located in eastern Turkey Gölalan Elazığ chromium deposits vertical magnetic anomaly is applied (figure 3). After applying the wavelet method to the land data, first the residual anomaly map is obtained and is shown in figure 3a. Subsequently, the wavelet method's detail coefficients were obtained. Horizontal, vertical and diagonal maps of the residual anomaly map are obtained in the detail coefficients. As a result, we can detect discontinuity boundaries by using various components related to wavelet transform and reveal structure boundaries. With this method it is possible to determine where the structures are located, to make suggestions for drilling there, or to reveal the reserves of the minefields.

Contributions

This research was supported by Research Institute of Istanbul University (The Project Number: 3823).

References

- [1]. Fedi, M. and Quata, T. (1998). Wavelet Analysis for the regional-residual and local seperstion at potential field anomalies. *Geophysical Prospecting*, 46, 507-525.
- [2]. Uçan, O.N., Şeker, S., Albora, A. M. and Özmen, A. (2000). Separation of Magnetic Field Data Using 2-D Wavelet approach. *Journal of the Balkan Geophysical Society*, 3, 53-58.
- [3]. Uçan, O.N. Albora, A.M. and Hisarlı, Z.M. (2001). Comments on the Gravity and Magnetic Anomalies of Saros Bay using Wavelet approach. *Marine Geophysical Researches*, 22, 251-264.



- [4]. Daubechies, L. (1990). The Wavelet Transform, Time-Frequency Localization and Singnal Analysis. IEEE Trans. on Information Theory, 36.
- [5]. Alp H., Albora A.M., Tur H. (2011). A View of Tectonic Structure And Gravity Anomalies of Hatay Region Southern Turkey Using Wavelet Analysis. Journal of Applied Geophysics, 75, 498-505.
- [6]. Oruç, B. (2014). Structural interpretation of south part of western anatolian using analytic signal of the second order gravity gradients and discrete wavelet transform analysis. Journal of Applied Geophysics, 103, 82-98.
- [7]. Albora, A.M and Uçan, O.N. (2001). Gravity Anomaly Separation Using 2-D Wavelet Approach and average depth calculate. Dogus Magazine-Dogus University, 3, 1-13.
- [8]. Albora, A. M., Hisarlı, Z. M. and Uçan, O. N. (2004). Application of Wavelet Transform to Magnetic Data Due to Ruins of Hittite Civilization in Turkey. Pure and Applied Geophysics, 161, 907-930.
- [9]. Alp, H. and Albora, A. M. (2009). Tracing of East Anatolian Fault Zone by using Wavelet analysis method. e-Journal of New World Sciences Academy Vol: 3, Issue: 2, Pages: 151-167.
- [10]. Albora A.M. (2014). Wavelet Method Approach of Archaeogeophysics Studies., Signal Processing and Communication Application Conference (SIU), 2016 22th, 514-517.
- [11]. Albora, A.M., Bal, A., Hisarli, Z.M., Ucan, O.N. (2008). A New Approach for Evaluation of Ruins of Hittite Civilization: Wavelet-Cellular Neural Network (Wave-CNN). Current Development in Theory and Applications of Wavelets. 2,3, 229-252.
- [12]. Albora, A.M. (2016). Wave-CNN Method Approach of Archaeogeophysics Studies. Signal Processing and Communication Application Conference (SIU), 2016 24th 173-176.
- [13]. Albora, A. M., Bal, A., Ucan, O. N. (2007). A new approach for border detection of Dumluca (Turkey) iron ore area: Wavelet Cellular Neural Networks. Pure and Applied Geophysics, 164, 119-215.
- [14]. Mallat, S.A. (1989). Theory for Multiresolution Signal Decomposition the Wavelet Representation, IEEE Trans. Pattern Anal. and Machine Intelligence, 31,679-693.
- [15]. Yungul S. (1956). Prospecting for chromate with gravimeter and magnetometer over rugged topography in East Turkey, Geophysics, 2, 433-454.
- [16]. Albora, A.M. Özmen, A. and Uçan., O.N. (2001). Residual Separation of Magnetic Fields Using a Cellular Neural Network Approach. Pure and Applied Geophysics, 158, 1797-1818.

